Suppressing Dissociation in Sonoluminescing Bubbles: The Effect of Excluded Volume

Ruediger Toegel, Sascha Hilgenfeldt, and Detlef Lohse
Department of Applied Physics and J. M. Burgers Centre for Fluid Dynamics, University of Twente, 7500 AE Enschede, The Netherlands

(Received 30 April 2001; published 2 January 2002)

Recent theoretical work in single-bubble sonoluminescence has suggested that water vapor in the collapsing bubble leads to energy-consuming chemical reactions, restricting the peak temperatures to values for which hardly any light emission could occur. Analyzing the reaction thermodynamics within the dense, collapsed bubble, we demonstrate that the excluded volume of the nonideal gas results in pronounced suppression of the particle-producing endothermic reactions. Thus, sufficiently high temperatures for considerable bremsstrahlung emission can be achieved.

DOI: 10.1103/PhysRevLett.88.034301 PACS numbers: 78.60.Mq

A violently collapsing gas bubble can emit short flashes of light so intense as to be visible to the naked eye. Stable clocklike light emission from an isolated gas bubble known as single-bubble sonoluminescence (SBSL) was first reported in 1990 [1] and has been studied extensively since [2–4]. The probable origin of SBSL light emission has been identified as thermal bremsstrahlung and recombination radiation from the optically thin bubble heated to a few 10^4 K peak temperature [5–8]. Recently, it has been pointed out that water vapor may significantly reduce the heating at collapse of the bubble [9–12]. Water vapor invades and escapes the bubble as it expands and collapses. However, the final phase of collapse is so fast that vapor cannot readily diffuse to the bubble wall to maintain the equilibrium composition. Thus, a considerable portion of vapor is trapped [10–12], which acts to reduce heating in two ways: (i) As the rest of the bubble consists largely of noble gas [13], the presence of water reduces the effective adiabatic exponent of the mixture, restricting the maximum temperature of the bubble to about 15 000–20 000 K [6,8,10,12]. These temperatures are nevertheless sufficiently high for thermal bremsstrahlung emission. (ii) Taking chemical reactions of the water vapor into account [9,14] drastically decreases the temperature since most of the reactions are endothermic and hence consume a major part of the thermal energy of the bubble. At the residual temperature of 6000–8000 K [10] hardly any thermal bremsstrahlung or recombination radiation would occur. These temperature calculations rely on chemical reaction rates and chemical equilibrium data that were taken under conditions much less extreme than those in a collapsed SBSL bubble, where the gas reaches almost solid state density. There is therefore some uncertainty about the quantitative results. In this Letter we attempt a more fundamental approach to obtain reaction rates for high-density gases. We find significant suppression of chemical reactions under typical sonoluminescence conditions, resulting in sufficiently high peak temperatures for light emission. Qualitatively, the mechanism at work is Le Chatelier's principle applied to a reactive van der Waals gas: dissociated water vapor molecules in the bubble take up more space than undissociated molecules. When the bubble volume becomes comparable to the excluded volume of the gas molecules, little free space remains, favoring the undissociated state.

Ansatz and crucial assumptions.—(i) Following the dissociation hypothesis [13,15] the incondensable gas in the bubble is assumed to be argon. In addition, water vapor and its chemical reaction products are taken into account. (ii) In a first step we consider as an example of a particle-producing reaction the dissociation of water into H and OH radicals.

$$H_2O + 5.1\ \text{eV} \leftrightarrow OH + H. \tag{1}$$

(iii) As in [12] we assume a hard-sphere potential for the molecular interaction with a common excluded volume $B \approx 5.1 \times 10^{-29}\ \text{m}^3$ [16] for all species. (iv) We define the zero energy level as the energy of an OH radical at rest. In this frame of reference an H_2O molecule, unlike the other species, has an additional potential energy $E_b = 5.17$ eV due to the H-OH bond energy. (v) The various internal degrees of freedom of the molecules, i.e., rotations and vibrations, do not couple. (vi) Electronic excitation is negligible compared to the other degrees of freedom, so that only the statistical weight of the electronic ground state needs to be taken into account. (vii) The formalism described below leads to a van der Waals correction to the reaction equilibrium constant of (1). Because of the common value of B, the same correction can then be applied to all particle-producing reactions in a more elaborate scheme taken from Refs. [9,14], consisting of eight forward and backward reactions.

Partition function.—The partition function of the bubble contents is [17,18]

$$Z = \frac{\xi_{H_2O}^{N_{H_2O}}}{N_{H_2O}!}\frac{\xi_{OH}^{N_{OH}}}{N_{OH}!}\frac{\xi_{H}^{N_{H}}}{N_{H}!}\frac{\xi_{Ar}^{N_{Ar}}}{N_{Ar}!}\left(1 - \frac{NB}{V}\right)^N. \tag{2}$$

Here $N = N_{Ar} + N_{H_2O} + N_{OH} + N_H$ is the total number of particles in the bubble, T is its temperature, and V is its volume. The factors ξ_X are perfect gas partition functions for single particles of species X, namely [17,18],

$$\xi_X = g_X V/\lambda_X^3 \quad \text{for } X = \text{Ar}, \text{H}, \tag{3}$$

© 2002 The American Physical Society

$$\xi_{\mathrm{OH}} = g_{\mathrm{OH}} V/\lambda_{\mathrm{OH}}^3 \frac{T}{\gamma_{\mathrm{OH}}\theta_{r,\mathrm{OH}}(1 - e^{-\theta_{v,\mathrm{OH}}/T})}, \tag{4}$$

$$\xi_{\mathrm{H_2O}} = g_{\mathrm{H_2O}} V/\lambda_{\mathrm{H_2O}}^3 e^{E_b/kT} \times \left(\frac{\pi T^3}{\gamma_{\mathrm{H_2O}}^2 \prod \theta_{r,\mathrm{H_2O},i}}\right)^{1/2} \frac{1}{\prod(1 - e^{-\theta_{v,\mathrm{H_2O},i}/T})}, \tag{5}$$

where $\lambda_X = h/(2\pi m_X kT)^{1/2}$, with the Planck and Boltzmann constants h and k, and the masses m_X of single X particles. The constants g_X are statistical weights of the electronic ground state; γ_X characterize the molecular symmetry. $\theta_{r,X}$ and $\theta_{v,X}$ are characteristic rotational and vibrational temperatures, respectively (see Table I for numerical values).

Chemical equilibrium.—The chemical potentials of the various species in the bubble are readily calculated from $\mu_i = -kT\frac{\partial \ln Z}{\partial N_i}$. Applying the general condition for chemical equilibrium $\sum \mu_j \delta N_j = 0$ and bearing in mind that in reaction (1), $\delta N_{\mathrm{Ar}} = 0$, $\delta N_{\mathrm{H}} = \delta N_{\mathrm{OH}} = -\delta N_{\mathrm{H_2O}}$, we find $\mu_{\mathrm{OH}} + \mu_{\mathrm{H}} - \mu_{\mathrm{H_2O}} = 0$, or equivalently,

$$\frac{N_{\mathrm{OH}}^2}{N_{\mathrm{H_2O}}} = K_{eq} V = K_0 T V \frac{\prod(1 - e^{-\theta_{v,\mathrm{H_2O},i}/T})}{(1 - e^{-\theta_{v,\mathrm{OH}}/T})} e^{-E_b/kT} \times \left(1 - \frac{NB}{V}\right) e^{\frac{-NB}{V-NB}}, \tag{6}$$

where we used $N_{\mathrm{OH}} = N_{\mathrm{H}}$. The constant K_0 is given by

$$K_0 = \frac{g_{\mathrm{OH}} g_{\mathrm{H}} \gamma_{\mathrm{H_2O}}}{g_{\mathrm{H_2O}} \gamma_{\mathrm{OH}}} \left(\frac{m_{\mathrm{OH}} m_{\mathrm{H}} 2\pi k}{m_{\mathrm{H_2O}} h^2}\right)^{3/2} \left(\frac{\prod \theta_{r,\mathrm{H_2O},i}}{\pi \theta_{r,\mathrm{OH}}^2}\right)^{1/2}. \tag{7}$$

Equation (6) is the law of mass action for a van der Waals gas. The last two terms are specific to the excluded-volume gas we are considering and lead to exponential suppression of dissociation under SBSL conditions when the particle density N/V approaches the critical value $1/B$. Note that the right-hand side of this equation—the equilibrium constant K_{eq}—is now density dependent and (6) hence becomes implicit. Only in the low-density limit it reduces to the formula for a perfect gas. Equation (6) is known in chemistry as the extension of the Guldberg and Waage law of mass action to real gases [19]. It can also be derived by means of the partial fugacities of a van der Waals gas.

Figure 1 plots the equilibrium constant K_{eq} as a function of temperature for different excluded volume fractions NB/V. With increasing density one observes a shift towards lower values, equivalent to suppression of dissociation. The circles show for comparison the values taken from [20].

TABLE I. Numerical values of the material constants in the partition function [18]. Note also $g_{\mathrm{Ar}} = 1$, $g_{\mathrm{H}} = 2$.

Species	i	$\theta_{r,X,i}$/K	$\theta_{v,X,i}$/K	g_X	γ_X
H_2O	1	13.37	2295	1	2
	2	20.87	5255		
	3	40.00	5400		
OH	1	27.18	5370	4	1

We now incorporate high-density reaction thermodynamics into the model of Ref. [12] in order to evaluate the effects of excluded volume on temperature and composition of a typical SBSL bubble. Because of the simplifications in the model, the results should be understood as approximative, but they show a robust trend.

Bubble dynamics.—The Keller-Miksis equation [21] is used as an equation of motion for the bubble wall radius R. The pressure p_g inside the bubble is obtained from Z by $p_g = kT\frac{\partial \ln Z}{\partial V} = \frac{NkT}{V-NB}$. The remaining task is to determine the state variables N and T, as shown in the following paragraphs.

Mass and heat transport.—As the concentration of reaction products at the interface is orders of magnitude less than the argon concentration [10] its contribution to the total particle density and hence its influence on the transport parameters is small. We can thus model the changes in particle number by mass diffusion $\dot{N}^d$ and the diffusive heat losses $\dot{Q}$ using the same boundary layer formalism as in [12],

$$\dot{N}^d_{\mathrm{H_2O}} = 4\pi R^2 D \frac{n_{\mathrm{H_2O},0} - n_{\mathrm{H_2O}}}{l_d},$$

$$l_d = \min\left(\sqrt{\frac{RD}{|\dot{R}|}}, \frac{R}{\pi}\right),$$

$$\dot{Q} = 4\pi R^2 \kappa \frac{T_0 - T}{l_{th}}, \qquad l_{th} = \min\left(\sqrt{\frac{R\chi}{|\dot{R}|}}, \frac{R}{\pi}\right).$$

Here, $n_{\mathrm{H_2O},0}$ and T_0 are the equilibrium values of the water vapor number density and bubble temperature, and κ, χ are the thermal conductivity and thermal diffusivity for the gas mixture. We have given only $\dot{N}^d_{\mathrm{H_2O}}$ because diffusive

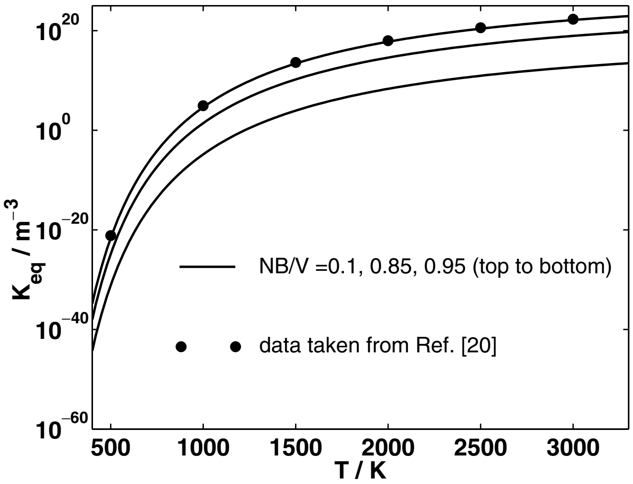

FIG. 1. The equilibrium constant K_{eq} for water dissociation as a function of temperature for different excluded volume fractions NB/V. As the latter is increased the equilibrium constant shifts to lower values, i.e., it favors the undissociated state. For comparison, the circles show values from the extensive data base gri_mech [20].

transport for other species is negligible. For further details, we refer to Ref. [12].

Reaction scheme.—We focus on reactions no. 1–8 of [9,14], involving the species Ar, H_2O, OH, H, O, H_2, and O_2, as species such as H_2O_2 and HO_2 are reported to appear only in trace amounts [10]. Since the forward and backward reaction rates (k_f, k_b) are related through their equilibrium constant [22] all rate constants of reactions of the type $A \rightarrow B + C$ are corrected for high density such that

$$K_{eq} = k_f/k_b \propto \left(1 - \frac{NB}{V}\right) e^{-NB/V - NB}, \tag{8}$$

where $N = \sum_X N_X$ is the total number of particles. Note that there is some ambiguity in how to distribute the correction factor among the forward and backward reaction rates. The result however is found to be independent of how this is done. This is mainly because the bubble contents remain at thermochemical equilibrium during collapse and hence only the equilibrium constant, i.e., the ratio k_f/k_b, matters.

Temperature.—Using once more the partition function, the total energy E of the bubble and its change with respect to time are found to be

$$E = kT^2 \frac{\partial \ln Z}{\partial T}, \tag{9}$$

$$\dot{E} = \sum_X \frac{\partial E}{\partial N_X} \dot{N}_X + \frac{\partial E}{\partial T} \dot{T} + \frac{\partial E}{\partial V} \dot{V}. \tag{10}$$

Note that, since more species are involved now, $\partial E/\partial T$ and $\sum_X \frac{\partial E}{\partial N_X} \dot{N}_X$ have been generalized accordingly. The latter expression is computed using

$$\sum_X \frac{\partial E}{\partial N_X} \dot{N}_X = \sum_j r_j \Delta E_j, \tag{11}$$

where r_j is the net reaction rate of elementary reaction j and ΔE_j is the corresponding reaction energy (including the difference of degrees of freedom of the initial and final states). The r_j are obtained from $k_{f,j}, k_{b,j}$ and the densities of particle species participating in reaction no. j. The binding energies and characteristic temperatures necessary to compute $\partial E/\partial T$ and the ΔE_j have been taken from [16,18].

Comparing (10) to the first law of thermodynamics for an open system [23], $\dot{E} = \dot{Q} - p_g \dot{V} + h_w \dot{N}_d$, and rearranging for $\dot{T}$ yields the differential equation for T necessary to close the model. Here $h_w \approx \frac{8}{2} kT_0$ is the molecular enthalpy of water vapor at the (cold) bubble wall.

Figure 2 depicts the dynamics of the fraction of vapor + reaction products $\zeta = (N - N_{Ar})/N$ and the temperature T for a time span of 6 ns around collapse for typical SBSL conditions. The high-density correction of the reaction rates leads to a suppression of reaction products. Accordingly, as the particle production is energy consuming, the peak temperature rises substantially, from ≈7000 to ≈10 000 K (Fig. 2b).

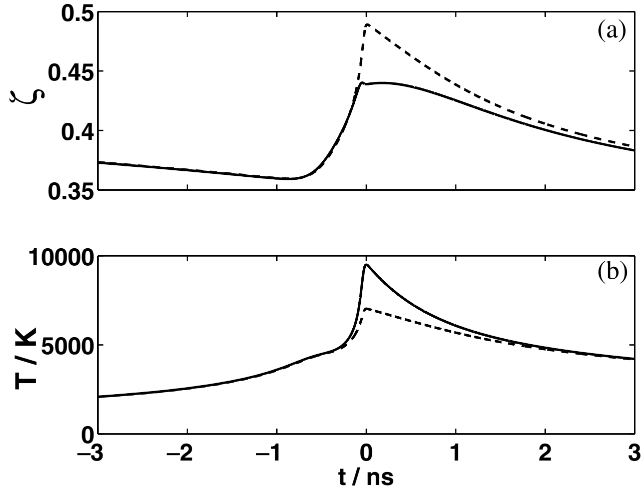

FIG. 2. (a) The combined fraction of vapor molecules + reaction products in an oscillating SBSL bubble as a function of time around collapse. (b) Bubble temperature for the same time interval. Dashed lines show calculations omitting excluded volume effects; solid lines correspond to the corrected reaction rates. The excluded volume correction raises the maximum temperature. The equilibrium radius is $R_0^{Ar} = 5$ μm, the driving pressure $P_a = 1.4$ bar, the liquid temperature $T_0 = 293.15$ K, and the driving frequency $f = 20$ kHz.

At the very moment of collapse the density in the bubble becomes so high that the model predicts recombination of already dissociated molecules, witnessed by the small dip of the ζ curve in Fig. 2a. Whether this feature reflects reality remains unclear as the recombination phase lasts for only ~100–200 ps; the validity of thermochemical equilibrium on this time scale is not obvious.

Figure 3 shows ζ^* and T^*, the fraction of vapor + reaction products and the temperature at the very moment of collapse, for different P_a. The argon content of the bubble was fixed (ambient radius $R_0^{Ar} = 5$ μm). In both

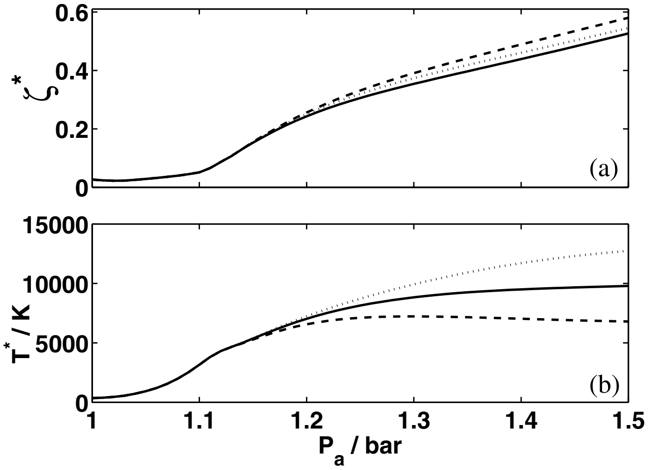

FIG. 3. Fraction of vapor + reaction products (a) and temperature (b) at the time of collapse as a function of the driving pressure amplitude (T_0, f, and R_0 as in Fig. 2). Dashed lines stem from the model without excluded volume effects; solid lines show corrected rates. In addition, the plot shows the results obtained using the inertially corrected Rayleigh-Plesset equation of Ref. [24] (dotted lines).

models ζ^* grows as the driving pressure is increased; the absolute numbers, however, differ. For $P_a = 1.5$ bar, e.g., the uncorrected model predicts $\zeta^* = 0.58$, whereas the corrected rates yield only $\zeta^* = 0.52$. This translates to 25% fewer particles in the bubble and, correspondingly, significantly enhanced temperatures. Neglecting the high-density correction leads to a maximum temperature of $T^* \approx 7000$ K around 1.25–1.3 bar. As P_a is further increased T^* drops again due to the dominant role of chemical dissociation. If, on the other hand, the excluded volume effect on the equilibrium constant is taken into account, the temperature is found to monotonically increase with P_a, until at $P_a = 1.5$ bar we find 10 000 K rather than 7000 K.

A more sophisticated model of bubble dynamics [24] takes inertial effects of the gas in the bubble into account. The gas pressure at the bubble wall $\tilde{p}_g$ in this case becomes

$$\tilde{p}_g = p_c - \tilde{\rho} R \ddot{R}/2, \tag{12}$$

where $\tilde{\rho}$ is the mean mass density of the gas mixture and p_c is the center pressure, respectively. Interpreting p_g as the mean gas pressure and using (12), stronger compression is achieved, and the excluded-volume effect described here is more pronounced. Temperatures of up to 13 000 K are found then (see the dotted line in Fig. 3).

In conclusion we propose a mechanism that, when combined with recent SBSL models [10,11], predicts temperatures high enough for light emission, even when the endothermic reaction chemistry of water vapor is taken into account. Because of the vanishing free volume as the bubble approaches maximum compression, the particle-producing dissociation reactions are found to be suppressed by Le Chatelier's principle for the excluded volume gas, to a degree far beyond what could be expected in an ideal gas.

Finally note that this result has bearing on high-density reaction thermodynamics beyond SBSL. For instance, empirical chemical reaction rates, obtained from hydrogen flame studies [25], should not be extrapolated via a modified Arrhenius law into a regime where the finite size of the particles becomes important.

This work is part of the research program of FOM, which is financially supported by NWO.

[1] D. F. Gaitan, Ph.D. thesis, The University of Mississippi, 1990.
[2] L. A. Crum, Phys. Today **47**, No. X, 22 (1994).
[3] B. P. Barber, R. A. Hiller, R. Löfstedt, S. J. Putterman, and K. R. Weninger, Phys. Rep. **281**, 65 (1997).
[4] D. Hammer and L. Frommhold, J. Mod. Opt. **48**, 239 (2001).
[5] B. Gompf, R. Günther, G. Nick, R. Pecha, and W. Eisenmenger, Phys. Rev. Lett. **79**, 1405 (1997).
[6] W. Moss, D. Clarke, and D. Young, Science **276**, 1398 (1997).
[7] S. Hilgenfeldt, S. Grossmann, and D. Lohse, Nature (London) **398**, 402 (1999).
[8] W. C. Moss, D. A. Young, J. A. Harte, J. L. Levatin, B. Rozsnyai, G. B. Zimmerman, and I. H. Zimmerman, Phys. Rev. E **59**, 2986 (1999).
[9] K. Yasui, Phys. Rev. E **56**, 6750 (1997).
[10] B. Storey and A. Szeri, Proc. R. Soc. London A **456**, 1685 (2000).
[11] B. Storey and A. Szeri, Proc. R. Soc. London A **457**, 1685 (2001).
[12] R. Toegel, B. Gompf, R. Pecha, and D. Lohse, Phys. Rev. Lett. **85**, 3165 (2000).
[13] D. Lohse, M. P. Brenner, T. Dupont, S. Hilgenfeldt, and B. Johnston, Phys. Rev. Lett. **78**, 1359 (1997).
[14] V. Kamath, A. Prosperetti, and F. Egolfopoulos, J. Acoust. Soc. Am. **94**, 248 (1993).
[15] T. J. Matula and L. A. Crum, Phys. Rev. Lett. **80**, 865 (1998); J. A. Ketterling and R. E. Apfel, Phys. Rev. Lett. **81**, 4991 (1998).
[16] *CRC Handbook of Chemistry and Physics,* edited by D. R. Lide (CRC Press, Boca Raton, FL, 1991).
[17] T. L. Hill, *Introduction to Statistical Thermodynamics* (Addison-Wesley, Reading, MA, 1960).
[18] J. A. Fay, *Molecular Thermodynamics* (Addison-Wesley, Reading, MA, 1965).
[19] I. Prigogine and R. Defay, *Chemical Thermodynamics* (Longmans, Green, London, 1962).
[20] Gregory P. Smith, David M. Golden, Michael Frenklach, Nigel W. Moriaty, Boris Eiteneer, Mikhail Goldenberg, C. Thomas Bowman, Ronald K. Hanson, Soonho Song, William C. Gardiner, Jr., Vitali V. Lissianski, and Zhiwei Qin, http://www.me.berkeley.edu/gri_mech/
[21] J. B. Keller and M. Miksis, J. Acoust. Soc. Am. **68**, 628 (1980); A. Prosperetti and A. Lezzi, J. Fluid Mech. **168**, 457 (1986).
[22] W. C. Gardiner, *Gas-Phase Combustion Chemistry* (Springer-Verlag, New York, 2000).
[23] G. N. Hatsopoulos and J. Keenan, *Principles of General Thermodynamics* (Wiley, New York, 1965).
[24] H. Lin, B. Storey, and A. Szeri, J. Fluid Mech. **452**, 145 (2002).
[25] F. N. Egolfopoulos and C. K. Law, in *Twenty-Third Symposium (International) on Combustion, Orléans, France, 1990* (The Combustion Institute, Pittsburgh, PA, 1990), pp. 333–340.